Translational Oncology 14 (2021) 100897

Contents lists available at ScienceDirect

Translational Oncology

journal homepage: www.elsevier.com/locate/tranon

Original research

BPRDP056, a novel small molecule drug conjugate specifically targeting phosphatidylserine for cancer therapy

Yun-Yu Chen [1], Chen-Fu Lo [1], Tai-Yu Chiu [1], Chia-Yu Hsu [1], Teng-Kuang Yeh [1], Ching-Ping Chen, Chen-Lung Huang, Chung-Yu Huang, Min-Hsien Wang, Yu-Chen Huang, Hsuan-Hui Ho, Yu-Sheng Chao, Joe C. Shih, Lun K. Tsou *, Chiung-Tong Chen *

Institute of Biotechnology and Pharmaceutical Research, National Health Research Institutes, Zhunan, Miaoli 35053, Taiwan, ROC

ARTICLE INFO

Article history:
Received 4 August 2020
Received in revised form 20 September 2020
Accepted 22 September 2020

Keywords:
BPRDP056
Dipicolylamine
Phosphatidylserine targeting
Drug conjugate
Drug delivery

ABSTRACT

Zinc(II)-dipicolylamine (Zn-DPA) has been shown to specifically identify and bind to phosphatidylserine (PS), which exists in bulk in the tumor microenvironment. BPRDP056, a Zn-DPA-SN38 conjugate was designed to provide PS-targeted drug delivery of a cytotoxic SN38 to the tumor microenvironment, thereby allowing a lower dosage of SN38 that induces apoptosis in cancer cells. Micro-Western assay showed that BPRDP056 exhibited apoptotic signal levels similar to those of CPT-11 in the treated tumors growing in mice.

Pharmacokinetic study showed that BPRDP056 has excellent systemic stability in circulation in mice and rats. BPRDP056 is accumulated in tumors and thus increases the cytotoxic effects of SN38. The *in vivo* antitumor activities of BPRDP056 have been shown to be significant in subcutaneous pancreas, prostate, colon, liver, breast, and glioblastoma tumors, included an orthotopic pancreatic tumor, in mice. BPRDP056 shrunk tumors at a lower (~20% only) dosing intensity of SN38 compared to that of SN38 conjugated in CPT-11 in all tumor models tested. A wide spectrum of antitumor activities is expected to treat all cancer types of PS-rich tumor microenvironments. BPRDP056 is a first-in-class small molecule drug conjugate for cancer therapy.

Introduction

Cancer is a major public health issue worldwide and a leading cause of death [1]. The anticancer chemotherapeutic drugs have serious systemic adverse effects, thus limiting their dosages and applications. Among the conventional cancer treatments, cancer chemotherapeutic drugs are given systemically and distributed throughout the whole body without specific targeting the tumors. To design therapeutics specifically targeting the cancer cells in tumors is a new strategy of drug development and has shown great promises [2,3]. Selective tumor targeting molecules, such as monoclonal antibodies [4] and specific biomarker-targeted small molecule compounds [5], have been incorporated into conjugates as the delivery systems for cytotoxic agents in drug development. Antibody-drug conjugates (ADCs) that utilize antibodies to deliver potent cytotoxic agents to diseased cells or cancer cells exhibit significant anticancer efficacies with reduced adverse toxicities of the cytotoxic agents. More than 50 distinct ADCs that target and utilize different kinds of targeting ligand heads, linkers, and cytotoxic agents are currently in clinical evaluations Polakis [6] and 4 ADCs have been approved for cancer patient uses [2,7]. However, ADCs have limitations such as those related to molecular size, intracellular penetration or pharmacokinetic issues as delivery system for cytotoxic drugs [8,9]. Small molecule drug conjugates (SMDCs) have therefore been proposed as a viable alternative to ADC for tumor-targeted drug delivery [10].

A SMDC consists of three components, *i.e.*, a molecule targeting head, a linker with a cleavable site, and a cytotoxic drug. The molecule targeting head in SMDC is of low molecular weight that contrasts to the molecule-targeting antibody in an ADC. An ideal linker is stable to conjugate the cytotoxic drug in the circulation system *in vivo* and preventing the cytotoxic drug from being released out of the whole conjugate before arriving at the tumor microenvironment area. Several approaches using SMDCs for treating cancer diseases are being investigated in preclinical and clinical studies [10]. Phosphatidylserine (PS) is abundant component phospholipids on the extracellular of dying and dead cells in the tumor microenvironment and thus serves as a tumor-selective biomarker for a targeting delivery mechanism [11]. Zinc(II)-dipicolylamine (Zn-DPA) coordination complexes have been described with strong binding affinity to PS [12–15]. Fluorochrome-conjugated Zn-DPA and radiolabeled Zn-DPA complexes can specifically accumulate the emitting signals in the xenografted prostate and mammary tumors in animals [16,17].

* Corresponding authors.
E-mail addresses: kelvintsou@nhri.edu.tw, (L.K. Tsou), ctchen@nhri.edu.tw. (C.-T. Chen).
[1] Yun-Yu Chen, Chen-Fu Lo, Tai-Yu Chiu, Chia-Yu Hsu and Teng-Kuang Yeh contributed equally to this work.

http://dx.doi.org/10.1016/j.tranon.2020.100897

CPT-11 (irinotecan, 7-ethyl-10-[4-(1-piperidino)-1-piperidino] carbonyloxycamptothecin) is an approved drug for the treatment of metastatic colorectal cancer worldwide, and in some countries for gastric cancer, non-small cell lung cancer, small cell lung cancer, cervical cancer, and non-Hodgkin's lymphoma. CPT-11 is a water-soluble prodrug that can be converted into SN38 (7-ethyl-10-hydroxycamptothecin), a topoisomerase I inhibitor and cytotoxic to cancer cells [18]. CPT-11 causes adverse toxicities at a higher dosage, which limits its therapeutic safety window [19].

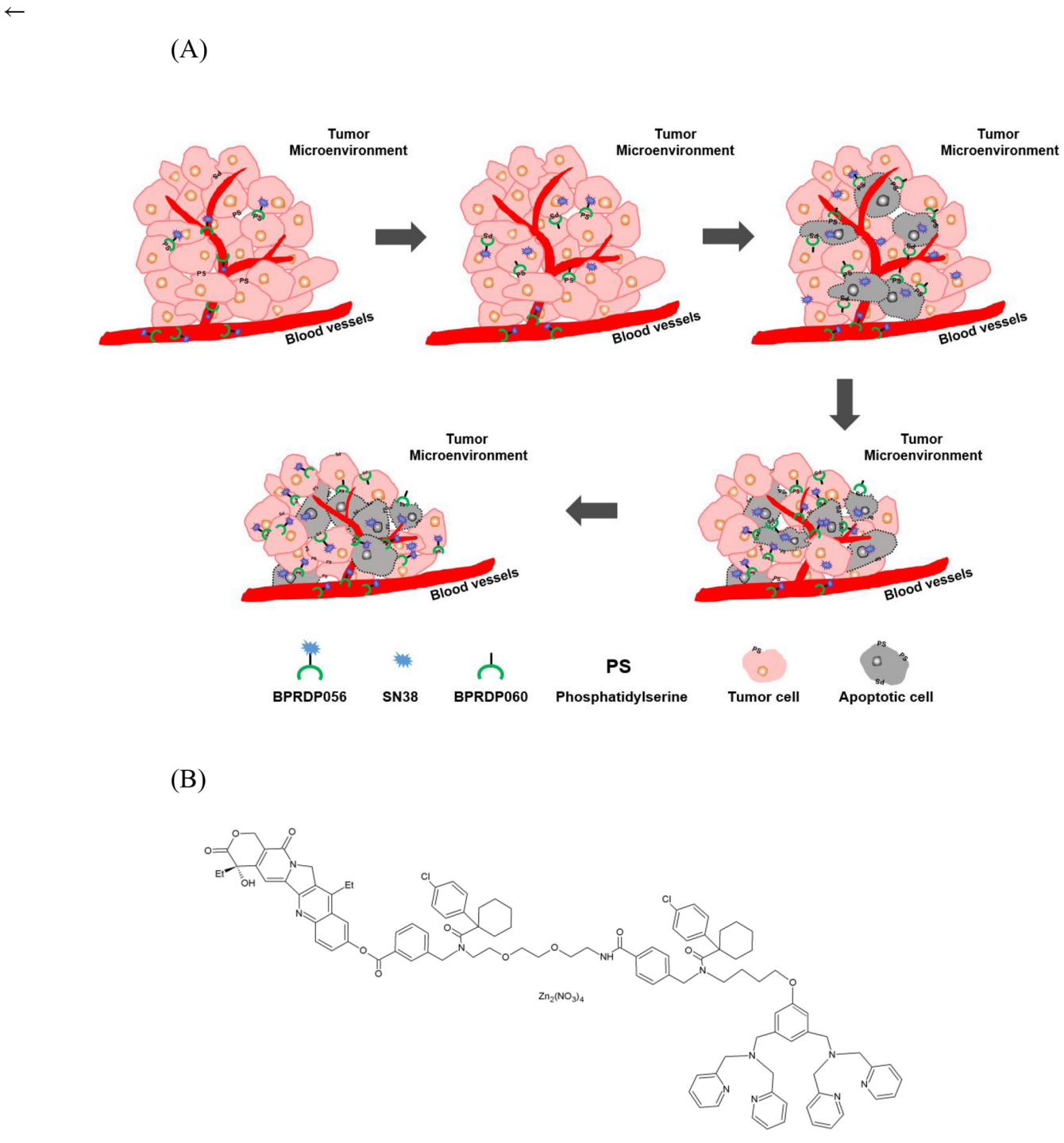

Fig. 1. Schematic illustration of the positive feedback mechanism of antitumor action by PS-targeting BPRDP056; chemical structures of BPRDP056, BPRDP067 and BPRDP060. (A) The diagram showing that BPRDP056 delivered *via* systemic circulation, diffused passively into tumor microenvironment and accumulated there in by targeting to PS molecules on tumor cells; release of cytotoxic SN38 due to enzyme-mediated cleavage *in situ*; apoptosis of the tumor cells caused by cytotoxic SN38 and more PS exposed led to more BPRDP056 accumulated and thus more SN38 released; tumor shrinkage due to apoptotic tumor cells disappeared after BPRDP056 treatment enhancing more PS exposed to recruit more BPRDP056 conjugates; and more tumor cells become apoptotic and eliminated resulting in further tumor shrinkage. BPRDP056 (B) and BPRDP067 (C) share similar chemical structures of which BPRDP067 lacks of the PS-specific targeting ability. BPRDP060 (D) has the same PS-specific targeting structure as that of BPRDP056 without the payload SN38.

Recently, a liposomal formulation of CPT-11, ONIVYDE® (PEP02, MM-398) was found to exhibit a longer systemic stability and reduced toxicities while maintaining its anti-tumor potency as a therapeutic option for treating pancreatic cancer [20].

BPRDP056 is a novel SMDC consisted of a designed linker connecting Zn-DPA with cytotoxic payload SN38. The linker in BPRDP056 does not mask the PS-specific tumor targeting ability of Zn-DPA, while simultaneously prohibit SN38 from its toxicity before being released free. A positive feedback of antitumor activities due to the PS-targeting mechanism, cytotoxic SN38 release, and therefore apoptotic induction has been hypothesized in Fig. 1A. In the present study, the potentials of BPRDP056 as a cancer therapeutic SMDC were investigated. Pharmacokinetic studies were carried out to measure BPRDP056 levels in the circulation system in mice and rats as well as in the tumors in mice. Antitumor activities of BPRDP056 were evaluated in human pancreatic, prostate, colorectal, hepatocellular, and breast carcinoma and glioblastoma in subcutaneous tumor xenograft and orthotopic human pancreatic tumor in mice.

Materials and methods

BPRDP056 and compounds

BPRDP056 (Fig. 1B) consists of three parts: Bis (zinc-dipicolylamine) (Zn-DPA), which serves as an anchoring group to target PS; SN38, an antitumor bioactive compound; and a spacer-bridging moiety, a linker, between the first two parts. The linker predicts to have an AEBSF-sensitive enzyme digested cutting site and prevents the cytotoxic SN38 from being released out of the conjugate before arriving at the tumor microenvironment area [21]. BPRDP067 (Fig. 1C) is a conjugate of BPRDP056 analog lacking PS-specific targeting ability of DPA. BPRDP060 (Fig. 1D) has the same PS-specific targeting chemical structure as that of BPRDP056 without the payload SN38. CPT-11 (irinotecan, Herocan, Nang Kuang Pharmaceutical Co., Tainan, Taiwan), SN38 (7-ethyl-10-hydroxycamptothecin, ScinoPharm, Tainan, Taiwan), paclitaxel (71111AA071, ScinoPharm Taiwan), temozolomide

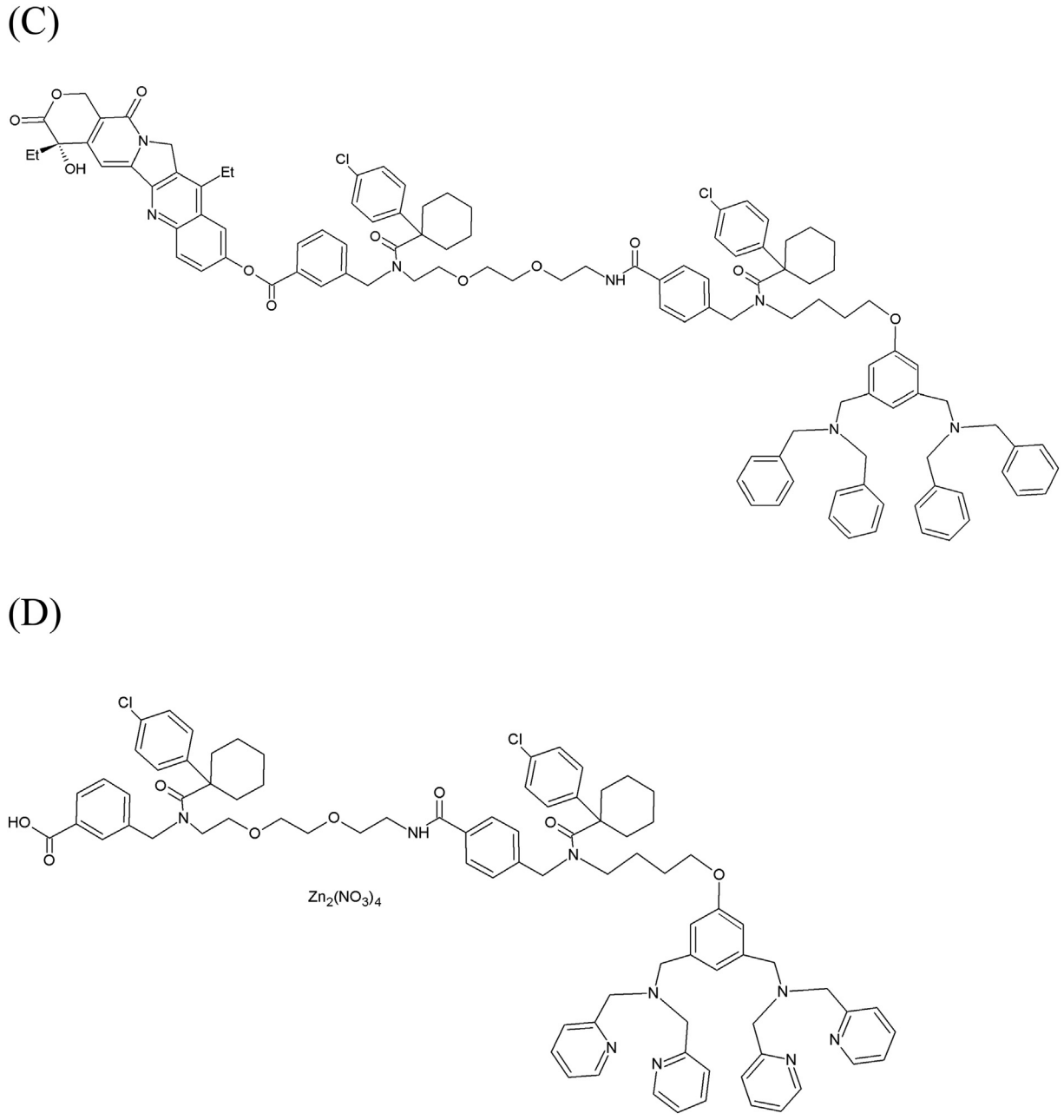

Fig. 1 (*continued*).

(PHR1437-1G, Sigma-Aldrich), and sorafenib (A10001-100, Adooq Bioscience LLC, Irvine, CA, USA) were purchased.

Cells and culture medium

Hep G2 (HB-8065) and U-87 MG (HTB-14) cells were from American Type Culture Collection (ATCC, Rockville, MD, USA). PC-3 (60122), COLO 205 (60054), MIA PaCa-2 (60139), and MDA-MB-231 (68014) cells were from the Bioresource Collection and Research Center (BCRC, Hsinchu, Taiwan). BxPc3-luc2 Bioware® cells were purchased from Caliper Life Sciences (Hopkinton, MA, USA). RPMI 1640 (31800-022), phenol red free RPMI 1640 (11835-030), minimum essential medium (MEM, 41500-034), Leibovitz's L-15 (41300-039), Dulbecco's Modified Eagle Medium (DMEM, 31600-034), phenol red free DMEM (21063-029) and horse serum (16050-122) were all from Thermo Fisher Scientific (Waltham, MA, USA) and Kaighn's Modification Ham's F-12 (HFP06-10X1LT) was from Caisson (North Logan, UT, USA). Fetal bovine serum (FBS, 04-001-1A-US) and Dulbecco's phosphate buffered saline (DPBS, 10×, 02-023-5A) were from Biological Industries (Beit Haemek, Israel). All cells were cultured in a humidified CO_2 incubator at 37 °C for uses.

Use and care of animals

Animals used for the studies were as follows: 6– 9-week-old male athymic NU-Fox1^{nu} nude and female severe combined immunodeficient (SCID) mice for xenograft, pharmacokinetic and micro-Western array studies; and 6– 9-week-old ICR mice and 6– 9-week-old male Sprague-Dawley (SD) rats for preliminary toxicity evaluations. All animals were purchased from BioLasco (Ilan, Taiwan) and housed in sterilized cages equipped with an air filter and sterile beddings at the AAALAC accredited facility, Laboratory Animal Center of the National Health Research Institutes (NHRI). Mice and rats were fed with sterilized water and chow *ad libitum* and kept under a 12-h light/12-h dark cycle throughout the study period. The experimental procedures and care of the animals were approved by the Institutional Animal Care and Use Committee of NHRI.

In vitro plasma stability study

Male ICR mice of 6-week-old were sacrificed, and the mouse blood samples were collected *via* cardiac puncture into EDTA tubes placed on ice. Plasma samples were obtained by centrifugation (3000 rpm for 15 min at 4 °C) and kept frozen at −20 °C until use. The plasma was subjected to *in vitro* compound stability study. The plasma aliquots of 70 μL were distributed to 0.6 mL microcentrifuge tubes (Basic Life, Taipei, Taiwan). BPRDP056 was dissolved in a mixture of DMSO and D5W (1:9, v/v) and 70 μL of the mixture each was added into the plasma tubes, followed by a 3-, 6- and 24-h incubation (n = 3 for each incubation time) at 37 °C in a water bath. The samples were measured for levels of BPRDP056 and SN38 released from cleavage of BPRDP056 by HPLC analysis.

Subcutaneous inoculation of tumor cells in mice and tumor size measurements

Cancer cells in culture were suspended in phenol red free medium/DPBS and mixed with Matrigel™ (356237, BD Biosciences, San Jose CA, USA) in 1:1 ratio. Individual mixtures of Matrigel™ with COLO 205 (1×10^6 cells), MIA PaCa-2 (1×10^6 cells), PC-3 (1×10^6 cells), Hep G2 (1×10^6 cells), U-87 MG (1×10^6 cells) and MDA-MB-231 (1×10^6 cells) cells were subcutaneously inoculated into the left flanks of mice using a 1 mL syringe (needle 24G × 1 in., 0.55 × 25 mm; TERUMO). Tumor dimensions were measured twice a week with an electronic caliper (FOW54-200-777, PRO-MAX, Newton, Massachusetts, USA) and the volume of the subcutaneously growing tumor in mm^3 was calculated by the formula: Volume = (length × width^2) / 2. Tumor-bearing mice were grouped by the averaged tumor sizes for treatments. Compound treatments were initiated when the mean tumor volume was approximately at 200–300 mm^3 for the anti-tumor study, 400–900 mm^3 for the measurements of compounds in the tumors study, and 300–400 mm^3 for the micro-Western study, respectively.

Compound treatments in mice with tumors growing subcutaneously tumors

Male nude mice of 6-week-old (Biolasco, Taiwan) were subcutaneously inoculated with human colorectal COLO 205, pancreatic MIA PaCa-2, prostate PC-3 and brain U-87 MG and liver Hep G2 cancer cells and female SCID mice of 6-week-old (Biolasco, Taiwan) were subcutaneously inoculated with breast cancer MDA-MB-231 cells to the left flanks, respectively. Treatment compounds were formulated as followings: BPRDP056 in 10% DMSO/20% Cremophor EL/70% injectable solution of 5% Dextrose (D5W) for treating COLO 205 and MIA PaCa-2 xenograft tumors; BPRDP056 in [Solutol HS 15:PEG400:Ethanol/5:2:3]:D5W = 1:4 for treating all the other tumors; BPRDP067 (a conjugate of BPRDP056 analog lacking PS-specific targeting ability of DPA) in 10% DMSO/20% Cremophor EL/70% D5W; BPRDP060 (DPA-linker only conjugate) in 10% DMSO/20% Cremophor EL/70% D5W; SN38 in 10% DMSO/20% Cremophor EL/10% Na_2CO_3/60% D5W; paclitaxel in 5% DMSO/20% Cremorphor EL/75% saline; sorafenib in 10% DMSO/20% Cremorphor EL/70% saline; and temozolomide in 10% DMSO/90% saline. The tumor-bearing mice were grouped and compound administrations were initiated when the mean tumor volume was approximately at 200–300 mm^3 in different dose regimens: BPRDP056 of 10 and 20 mg/kg and SN38 of 10 mg/kg at once daily for 5 consecutive days a week for 2 consecutive weeks with an interval of 2 non-dosing days (days 1–5 + days 8–12); BPRDP056 of 40 mg/kg, BPRDP067 of 40 mg/kg, CPT-11 of 40 mg/kg, and BPRDP060 of 33 mg/kg at twice (day 1 and day 4) a week for 2 weeks; paclitaxel of 20 mg/kg at once (day 1) a week for 2 weeks; sorafenib of 30 mg/kg orally gavaged daily in days 1–5 + days 8–12; temozolomide of 50 mg/kg orally gavaged daily for 5 consecutive days. Body weight of the mice and tumor volume were measured twice weekly.

Orthotopic implantation of pancreatic BxPc3-luc2 tumor cells in mice

Human pancreatic BxPc3-luc2 (5×10^6) cells per mouse were subcutaneously inoculated in male nude mice of 6-week-old. The growing tumors were harvested at a size of 500–600 mm^3, washed with cold PBS twice, minced into small pieces in PBS, mixed with Matrigel™ in a 1:1 ratio, and then injected orthotopically at 0.1 mL into the pancreas of the nude mice by using 1 mL syringe (needle 24G × 1 in., 0.55 × 25 mm; TERUMO). The subcutaneous and orthotopic tumors growing in mice were monitored for the reporter luciferase activities by an intraperitoneal injection of 150 mg/kg D-luciferin potassium salt (PerkinElmer, Waltham, MA, USA) to the mice followed by whole body images taking after 15 min of the luciferin injection by an IVIS Spectrum *in vivo* imaging system (Caliper Life Sciences, Hopkinton, MA, USA). The whole-body bioluminescence imaging and body weight of the mice were measured once weekly. The orthotopic tumor bearing nude mice were divided into 2 groups at 4 mice each when the luciferin intensity of the tumors in mice reached 5×10^7–5×10^8 photon/s on the third week after the BxPc3-luc2 cells implantation. BPRDP056 dissolved in [Solutol HS15:PEG400:Ethanol/5:2:3]:D5W = 1:4 was intravenously administered at 30 mg/kg twice a week for 4 weeks. A vehicle-administered control group was included for comparison.

Micro-Western array analysis of MIA PaCa-2 tumors

Male nude mice of 6-week-old were subcutaneously inoculated with 1×10^6 pancreatic cancer MIA PaCa-2 cells in the left flank. When the mean tumor volume was approximately at 300–400 mm^3, the mice were grouped at 4 mice each and a single intravenous dose of CPT-11 at 40 mg/kg, of BPRDP056 (dissolved in [Solutol HS 15:PEG400: Ethanol/5:2:3]:D5W = 1:4) at 40 mg/kg, and of vehicle ([Solutol HS 15:PEG400: Ethanol/5:2:3]:D5W = 1:4) was administered, respectively. The mice were euthanized at 48 h after the dosing and tumors were harvested

immediately for being homogenized in the lysis buffer [240 mM Tris-HCl, 1% (w/v) SDS, 0.5% (v/v) glycerol, 5 mM EDTA in H_2O] containing 1 mM DTT, 1 mM Na_3VO_4, 1% protease inhibitors (Sigma, P8340) and 1% phosphatase inhibitors (Sigma, P0044) by an electric homogenizer about 2–3 times, 10s per time, until homogenized completely. The tumor tissue lysates were collected by centrifuged at 13,000 rpm for 15 min at 4 °C and subjected to micro-Western Array [22] operated by Protein Chemistry Core Laboratory of the National Health Research Institutes, in which β-actin was used as an internal control. The protein expression levels of caspase-3, caspase-8, caspase-9, and *poly (ADP-ribose) polymerase* (PARP), cytochrome C and BCL-2 associated X (Bax) were measured. Heat map charts were generated to show the protein levels in ratios to that of β-actin control, normalized to vehicle control.

Pharmacokinetic study of BPRDP056

Pharmacokinetic study of BPRDP056 with intravenous injection of single dose (5 mg/kg) to ICR mice, repeated dose (30 and 50 mg/kg for 14-day repeated dose and 20 mg/kg once daily for 5 consecutive days in two consecutive dosing cycles with 2 non-dosed days in between) to SD rats and single dose (10 and 30 mg/kg) to tumor-bearing nude mice were studied. BPRDP056 was formulated in the mixture of [Solutol HS 15:PEG400:Ethanol/5:2:3]:D5W = 1:4 (v/v) for all pharmacokinetic studies.

Male ICR mice of 6-week-old (Biolasco, Taiwan) were divided into groups (n = 3 in each group) and intravenously administered with BPRDP056 at 5 mg/kg. At 0.003, 0.083, 0.25, 0.5, 1, 2, 4, 6, 8, and 24 h after dosing, the animals were sacrificed, and the blood sampling from each animal *via* cardiac puncture was collected in EDTA tubes and kept on ice and plasma samples were collected by centrifugation (3000 rpm for 15 min at 4 °C in a Beckman Model Allegra 6R centrifuge) and kept frozen at −20 °C until use.

BPRDP056 pharmacokinetic study in male SD rats was conducted using two different serial dose regimens: 30 and 50 mg/kg once daily for 14 consecutive days; and 20 mg/kg once daily for 5 consecutive days in two consecutive dosing cycles with 2 non-dosing days in between (days 1–5 + days 8–12). The rats were anesthetized with isoflurane inhalation and the blood samples were collected at 2–5 min and 30 min from the orbital sinus using capillary tubes, at 2, 24, 48, 120, and 168 h from the tail vein using a catheter, and at 192 h by cardiac puncture from 100% CO_2 euthanized rats after the last dosing. The rat blood samples were collected in Microtainer tubes with EDTA and centrifuged at 13,000 rpm for 10 min at 4 °C for plasma collection. Plasma samples were stored at −20 °C until use.

Male nude mice subcutaneously bearing MIA PaCa-2 tumors were intravenously administered with BPRDP056 (10, 30 mg/kg). The mice were sacrificed to collect blood and tumor samples at 2, 6, 24, 48, 72, 168, and 336 h after the compound administration. All blood samples collected in EDTA tubes were centrifuged at 13,000 rpm for 5 min at 4 °C for plasma collection. The harvested tumors were homogenized in water by electric homogenizer about 2–3 times, 10s/time, until homogenized completely. The tissue homogenates were collected by centrifuged at 13,000 rpm for 15 min at 4 °C. The collected plasma and tumor homogenate samples were kept at −80 °C until LC-MS/MS analysis.

LC-MS/MS analysis

The collected plasma or tumor homogenate samples of 50 μL were mixed with 100 μL acetonitrile completely. Supernatants of the mixtures were collected by centrifuged at 15,000 rpm for 15 min at 4 °C and 15 μL of it was injected for LC-MS/MS analysis. The LC-MS/MS system consisted of an Agilent 1200 series LC system and an Agilent ZORBAX Eclipse XDB-C8 column (5 μm, 3.0 × 150 mm) interfaced to an MDS Sciex API 4000Q tandem mass spectrometer equipped with an ESI in the positive-scanning mode. The MS/MS ion transitions monitored were *m/z* 901/125 and 393/349 for BPRDP056 and SN-38, respectively. A gradient separation profile was employed; mobile phase A consisted of 10 mM ammonium acetate aqueous solution containing 0.1% formic acid, and mobile phase B consisted of acetonitrile and eluted as min/% of mobile B: 0–1.5/10, 1.5–4.6/40, 4.7–6/10 with a flow rate of 1.5 mL/min.

Data analysis and statistics

Tumor growth inhibition (TGI) in percentage was determined by the formula: TGI (%) = (1 − T / C) × 100, where T indicates the mean tumor volume of the compound-treated group and C indicates the mean tumor volume of vehicle-treated control. All the data were expressed as the mean or mean ± standard error of the mean (SEM). Statistical differences between the tumor volumes of the vehicle-treated control and compound-treated groups were determined by using *ANOVA* and followed by *Student-Newman-Keuls* multiple comparison test (GraphPad Prism, San Diego, CA, USA).

Results

In vitro stability of BPRDP056 in mouse plasma

BPRDP056 was highly stable in the mouse plasma *in vitro* and only 1 to 2% of SN38 was released from BPRDP056 from 3 h up to 24 h of the incubation time (Table 1). The high stability of BPRDP056 in the mouse plasma suggests that BPRDP056 is not subject to cleavage of any significant levels by the enzymes resided in the systemic circulation after it is intravenously administered to the animals.

Pharmacokinetic parameters of BPRDP056 in mice and rats

In vivo systemic pharmacokinetic studies of BPRDP056 were performed in the ICR mice and SD rats. One single intravenous dose of 5 mg/kg BPRDP056 was given to the mice. Plasma concentrations of BPRDP056 and the active payload, released SN38 from BPRDP056 in the circulation were measured and the pharmacokinetic parameters such as clearance (CL), steady-state volume of distribution (V_{ss}), and area under the plasma concentration curve (AUC_{0-24h}) were estimated and shown in Table 2. The small V_{ss} of BPRDP056 at 0.2 L/kg indicates that its systemic distribution is limited to the circulation. A 43-fold difference in the AUC extremely high for the intact conjugate BPRDP056 verse the released SN38 within 24 h in circulation and a slow CL of BPRDP056 at 0.5 mL/min/kg, showing a significantly good *in vivo* stability of BPRDP056 in mice (Table 2).

Furthermore, plasma concentration profiles of BPRDP056 and its active payload SN38 after 14 consecutive days of BPRDP056 administration in rats are shown in Table 1. The concentrations of BPRDP056 and SN-38 (released from BPRDP056) slowly decreased in plasma and could be detected until 8 days after the last dosing in rats. Then the areas under the rat plasma BPRDP056 and SN-38 concentration time profiles (AUC) during the study were calculated (Table 2). The pharmacokinetic study also revealed a high AUC ratio of the intact conjugate to SN38 in circulation.

In the MIA PaCa-2 subcutaneously xenografted tumor plug PK study, after injection of BPRDP056 (10 and 30 mg/kg) and CPT-11 (10 mg/kg) in MIA PaCa-2-bearing mice, the concentrations of CPT-11 and SN38 released from CPT-11 rapidly decreased within 48 h in plasma and tumor (Fig. 2A and B). The concentration of BPRDP056 slowly decreased and maintained a detectable level up to Day 14 in plasma and tumor (Fig. 2C–F). SN38 released from BPRDP056 of 10 and 30 mg/kg was detected within 6 and 48 h in tumors, respectively, but was maintained to 72 h in plasma. The concentration of DPA-linker conjugate (BPRDP060) also decreased

Table 1
Stability of BPRDP056 in mouse plasma.

Incubation time, h	BPRDP056:SN38, %
3	99:1[a]
6	99:1
24	98:2

[a] Mean (n = 3) of the remaining compounds.

Table 2
Pharmacokinetic parameters of BPRDP056 in mice and rats.

Species	Mouse			Rat		
Regimen	Single dose			Days 1–5 + Days 8–12	14-day repeated dose	
Dose	5 mg/kg			20 mg/kg	30 mg/kg	50 mg/kg
Parameter[a]	CL (mL/min/kg)	V_{ss} (L/kg)	AUC_{0-24h} (ng/mL × h)	AUC_{0-24h} (ng/mL × h)	AUC_{0-24h} (ng/mL × h)	
BPRDP056[b]	0.5	0.1	201,324	569,269 ± 12,931	713,852 ± 22,450	1,200,095 ± 50,459
SN38[c]	0.3	0.1	5119	3489 ± 138	3900 ± 169	5839 ± 239

[a] Data are expressed as mean or mean ± SEM.
[b] Parameters estimated based on the plasma concentrations.
[c] Parameters estimated based on the plasma concentrations of the SN38 released from BPRDP056 into the circulation.

slowly and maintained a detectable level up to 14 days and was higher in plasma than tumor.

BPRDP056 is active against growths of tumors subcutaneously xenografted in mice

The *in vivo* therapeutic efficacy of BPRDP056 against the growth of human tumors has been demonstrated in immunodeficient mice subcutaneously bearing tumors of the pancreas, prostate, colon, liver, breast, and glioblastoma cancer cells and shown in Fig. 3. Both BPRDP056 and CPT-11 were conjugates or prodrugs of the anti-cancer payload SN38 and consisted of SN38 in 18% and 58%, respectively. Therefore, BPRDP056 (40 mg/kg, 4 doses at twice per week for two weeks) was given in a total dose of SN38 at 29 mg/kg (*i.e.*, 40 mg/kg/dose × 4 doses × 18% = 29 mg/kg). Similarly, BPRDP056 at 10, 20 mg/kg and CPT-11 at 40 mg/kg were equal to total doses of SN38 given at 18 (10 mg/kg × 10 doses × 18%), 36 (20 mg/kg × 10 doses × 18%), and 93 (40 mg/kg × 4 doses × 58%) mg/kg, respectively. Furthermore, SN38 itself was given in a total dose of 100 (10 mg/kg × 10 doses) mg/kg. CPT-11 and SN38 did not show significantly prolonged antitumor activities (Fig. 3A and B).

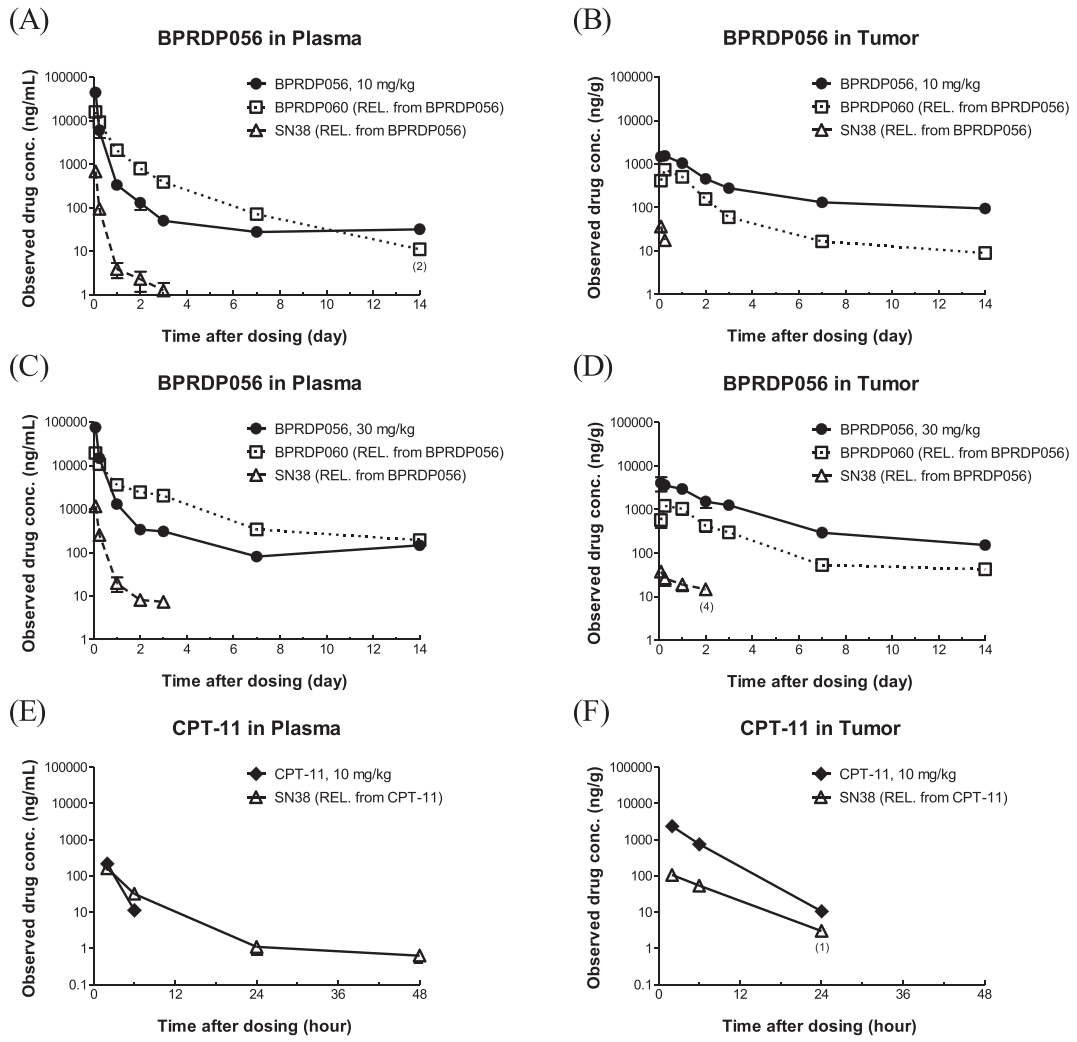

Fig. 2. Plasma and tumor levels of BPRDP056 and SN38 after one single dose of BPRDP056 in tumor-bearing mice. One single intravenous dose of BPRDP056 (10 and 30 mg/kg) or CPT-11 (10 mg/kg) was given to the nude mice with subcutaneously growing pancreatic MIA PaCa-2 tumors followed by plasma and tumor samples collections at the timepoints indicated. The remaining levels of BPRDP056 and concentrations of BPRDP060 (Zn-DPA-linker conjugate) and SN38 released from BPRDP056 in the plasmas (A, C) and tumors (B, D) were determined. The plasma and tumor concentrations of SN38 released from CPT-11 were also measured (E, F).

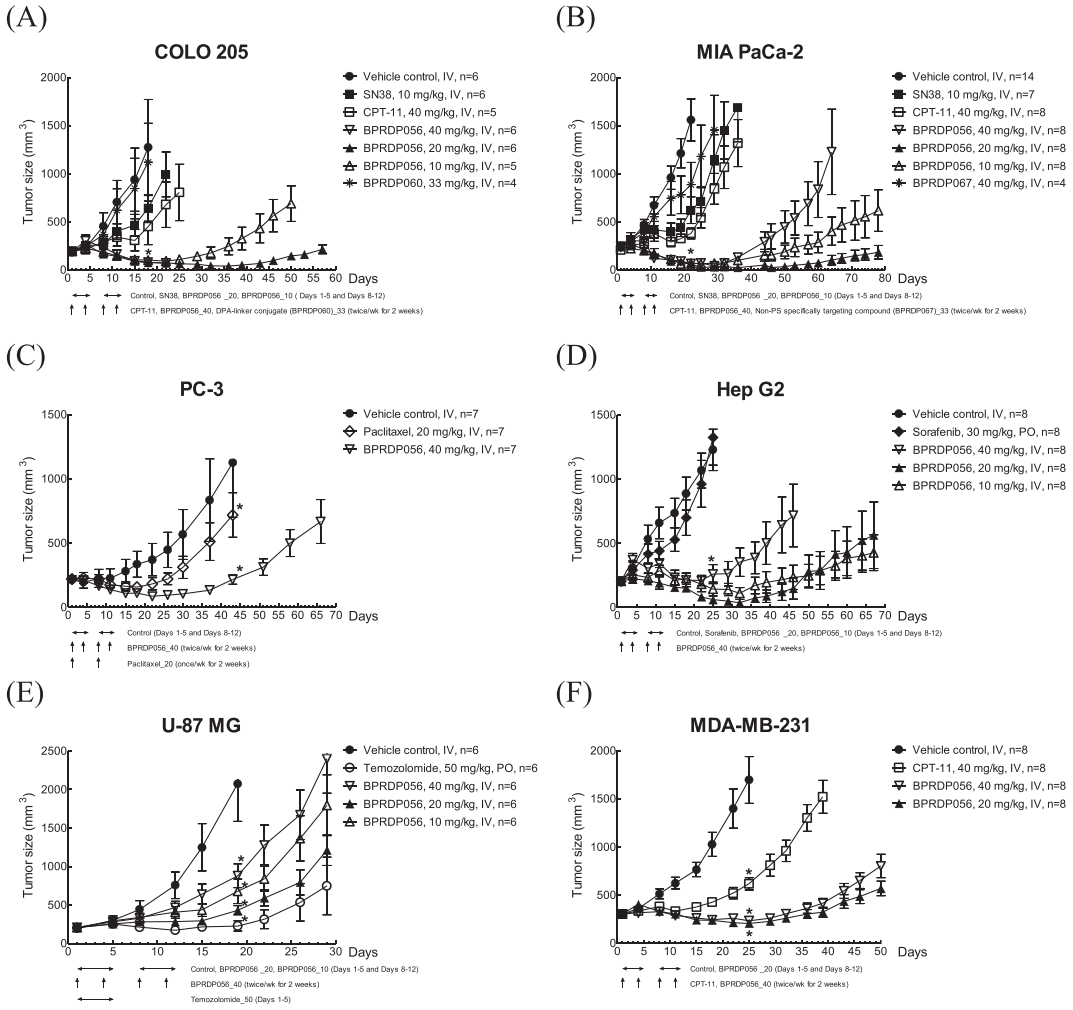

Fig. 3. *In vivo* activities of BPRDP056 against tumor growths in mice. BPRDP056 is active in a broad spectrum against human colorectal COLO 205 (A), pancreatic MIA PaCa-2 (B), prostate PC-3 (C), hepatocellular Hep G2 (D) and glioblastoma U-87 MG (E) tumor growths in male nude mice and breast MDA-MB-231 (F) tumor growths in female SCID mice. BPRDP056 of 10 and 20 mg/kg and SN38 of 10 mg/kg at once daily for 5 consecutive days a week for 2 consecutive weeks with an interval of 2 non-dosing days (days 1–5 + days 8–12); BPRDP056 of 40 mg/kg, BPRDP067 of 40 mg/kg, CPT-11 of 40 mg/kg, and BPRDP060 of 33 mg/kg at twice (day 1 and day 4) a week for 2 weeks; paclitaxel of 20 mg/kg at once (day 1) a week for 2 weeks; sorafenib of 30 mg/kg orally gavaged daily in days 1–5 + days 8–12; temozolomide of 50 mg/kg orally gavaged daily for 5 consecutive days. Data are expressed as the mean ± SEM. *: $p < 0.05$, treated *vs.* vehicle control by *ANOVA* followed by using the *Student-Newman-Keuls* test. Arrows indicate the timepoints of the dosing.

As shown in Fig. 3A, BPRDP056 in a dose-dependent manner exhibited significant activities against the growths and thus shrank the sizes of the human colorectal COLO 205 tumors in male nude mice compared to vehicle control (n = 4–6 mice per group). BPRDP056 was much more effective than SN38 and CPT-11 inhibiting the tumor growths in a total amount of BPRDP056-delivered payload SN38 much lesser than that of CPT-11 and SN38 itself. On the other hand, BPRDP060 (Fig. 1C), the part of DPA-linker conjugate of BPRDP056 without the active payload SN38, was intravenously given in 4 doses at 33 mg/kg each and did not show any antitumor activity in mice (Fig. 3A). A similar and significant dose-dependent antitumor activity of BPRDP056 was observed against the growths of human pancreatic MIA PaCa-2 tumors subcutaneously xenografted in male nude mice compared to vehicle control (n = 4–14 mice per group) as shown in Fig. 3B. BPRDP056 exhibited significant antitumor activities compared to vehicle control by a TGI of 96%, whereas CPT-11 showed a TGI of 75% only. Again, the total amount of SN38 delivered by BPRDP056 was less than 1/3 that given by CPT-11, and yet it resulted in more potent tumor growth inhibition, markedly, showing shrinkage in tumor size. BPRDP056 also caused prolonged tumor growth regression in all tumor-bearing mice, leaving one mouse each in the 2 treatment groups of 10 and 20 mg/kg free of tumors on day 78 and day 81, respectively, at the end of the observation period. Furthermore, BPRDP067 (Fig. 1C) has a chemical structure similar to BPRDP056, lacking of the PS-specific targeting ability. However, BPRDP067 did not exhibit significant antitumor growth activity (Fig. 3B) though it shares a similar amount of the active payload SN38 to that of BPRDP056. The *in vivo* PS-specific tumor targeting ability of an intact Zn-DPA on BPRDP056 is critical to elicit its *in vivo* antitumor activities in mice. BPRDP056 demonstrated similar dose-dependent antitumor activities in four other human tumors subcutaneously xenografted in immunodeficient mice shown in Fig. 3C (prostate PC3 tumor, n = 7 mice per group), Fig. 3D (liver Hep G2 tumor, n = 8 mice per group), Fig. 3E (U-87 MG glioblastoma, n = 6 nude mice per group), and Fig. 3F (breast MDA-MB-231 tumor, n = 8 female SCID mice per group). As the dose levels and regimens of the compound treatments were indicated in the individual figures, a few other reference drugs were included for comparisons as well such as paclitaxel, sorafenib and temozolomide. BPRDP056 showed significantly better antitumor activity than paclitaxel intravenously given at 20 mg/kg per week for 2 weeks (Fig. 3C). As noted, the Hep G2 tumors in 2 of the 8 male nude mice in each of the 3 dosing groups (10, 20, and 40 mg/kg) disappeared after BPRDP056 treatments and did not relapse till the end of the observation period (Fig. 3D). While showing dose-dependent antitumor activity, BPRDP056 at 20 mg/kg induced efficacy against human brain U-87

MG glioblastoma comparable to that by temozolomide at 50 mg/kg in nude mice (Fig. 3E). BPRDP056 intravenously administered at both regimens (20 mg/kg/day on days 1–5 + days 8–12; 40 mg/kg twice per week for two weeks) significantly shrank tumor size of the treated MDA-MB-231 tumors growing in female SCID mice (Fig. 3F). Overall, the antitumor activities of BPRDP056 are dose level-dependent and dose frequency-dependent against a broad spectrum of human tumor growths.

BPRDP056 inhibited the growth of pancreatic tumors orthotopically xenografted in mice

An orthotopic pancreatic tumor model was established by using the human tumor cell BxPC3-luc2 to evaluate the activity of BPRDP056 against pancreatic tumor growth in nude mice. The growing orthotopic BxPC3-luc2 tumors were monitored *in situ* by observing the change of the luciferin intensity in the whole-body imaging of the mice. BPRDP056 of 30 mg/kg given intravenously at twice a week for 4 weeks induced a delayed on-set (Day 21) and significant decrease in the luciferin intensity of the orthotopic BxPC3-luc2 tumors (Fig. 4A). While BPRDP056 significantly suppressed the growths of the orthotopic BxPC3-luc2 tumors, there was no significant difference in body weights of the mice compared to vehicle control (Fig. 4B). Representative whole body bioluminescence images of the orthotopic BxPC3-luc2 tumor-bearing mice, obtained by using an IVIS system before and after vehicle control or BPRDP056 treatments were shown in Fig. 4C.

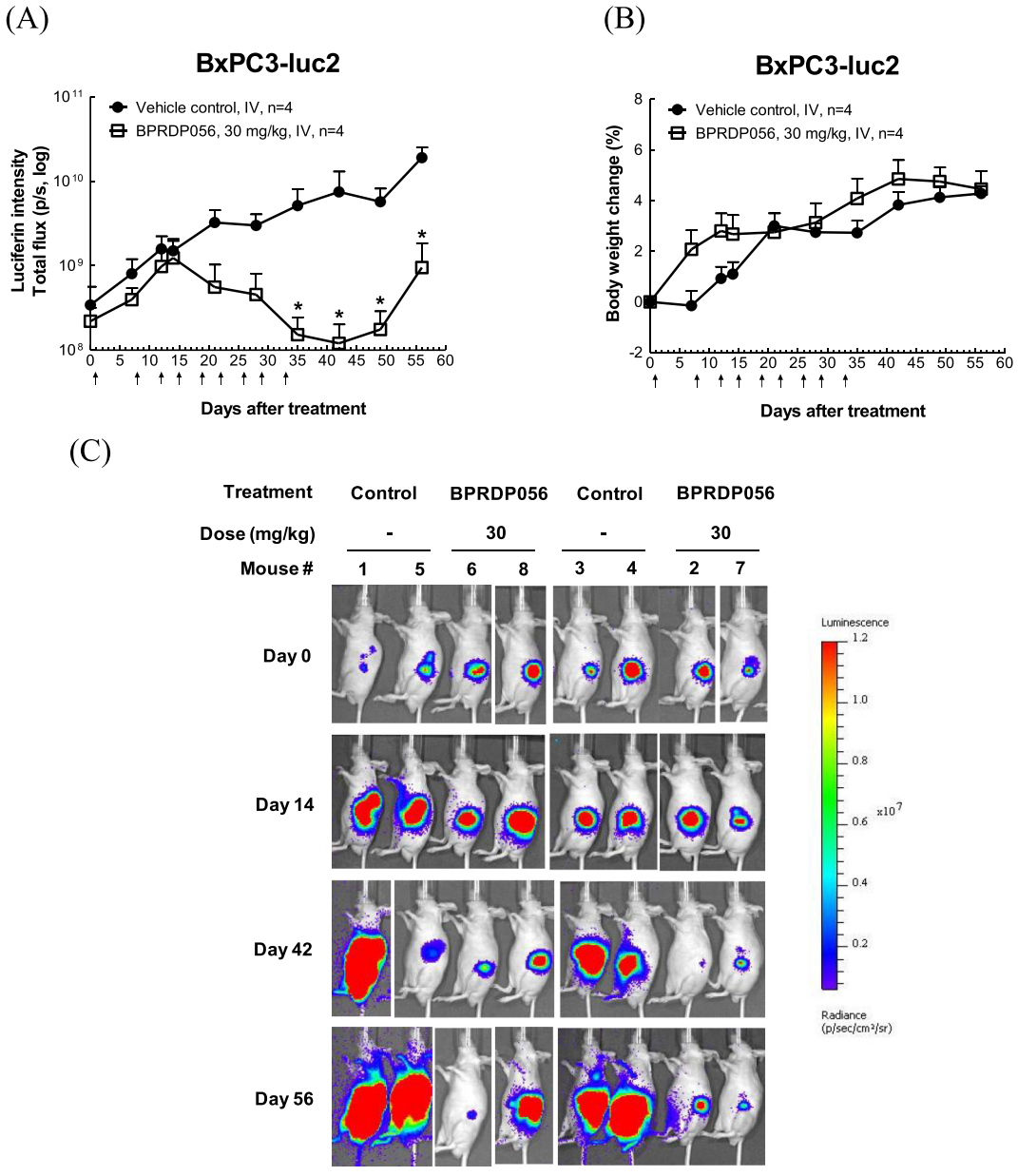

Fig. 4. *In vivo* activity of BPRDP056 against the orthotopic growth of human pancreatic tumors in mice. By observing the change in the luciferin intensity of the whole-body imaging of the mice, BPRDP056 treatments significantly shrunk the size of orthotopic growing pancreatic BxPC3-luc2 tumors (A) without causing significant difference in the body weights (B) in nude mice as compared to that of vehicle control. BPRDP056 of 30 mg/kg was intravenously administered once in the first week followed by twice a week for four consecutive weeks. Arrows indicate timepoints of the dosing. *: $p < 0.05$, BPRDP056-treated *vs.* vehicle control by using the *Student-Newman-Keuls* test. The volume of tumors of BxPC3-luc2 cancer cells growing in the pancreas of the nude mice were monitored by the bioluminescence intensity resulted from the reporter luciferase activities. The whole-body mages were taken at the days indicated with representative images shown (C).

BPRDP056 induced apoptotic cell death in pancreatic tumors growing in mice

The tumor tissues were harvested from the nude mice orthotopically bearing MIA PaCa-2 tumor in the pancreas of the mice intravenously administered with a single dose of BPRDP056 and CPT-11 at 40 mg/kg, respectively, and the protein abundances in the apoptotic pathways were measured. The apoptosis process in the treated tumors was verified. In the heat map chart (Fig. 5), black indicates no change, while red and green indicate increases and decreases, respectively, in the levels of the selective apoptosis-related proteins. In the tumors of BPRDP056 treated, the levels of caspase-3, caspase-8, caspase-9, and PARP, cytochrome C and Bax were found to be significantly increased. Micro-Western assays showed that BPRDP056 exhibited apoptotic cell death signal profiles similar to those of CPT-11 in the treated tumors in mice as shown in Fig. 5. With the same active payload SN38 conjugated, BPRDP056 shared the same apoptosis mechanism with CPT-11 for their antitumor activities.

Discussion

PS is an anionic phospholipid component of the inner leaflet of the cell membrane in all eukaryotic cells. Oxidative stress results in the exposure of PS on the outer surface of the tumor cells and tumor vessel endothelium in tumor microenvironment. PS has been suggested as a biomarker for a number of human tumors such as lung, breast, pancreatic, bladder, skin, brain and rectal adenocarcinoma, but not in healthy cells [22]. Bavituximab is an unconjugated, chimeric immunoglobulin G1 (IgG1) monoclonal antibody directed to bind PS-binding protein beta 2 glycoprotein-1 (β2GP1)

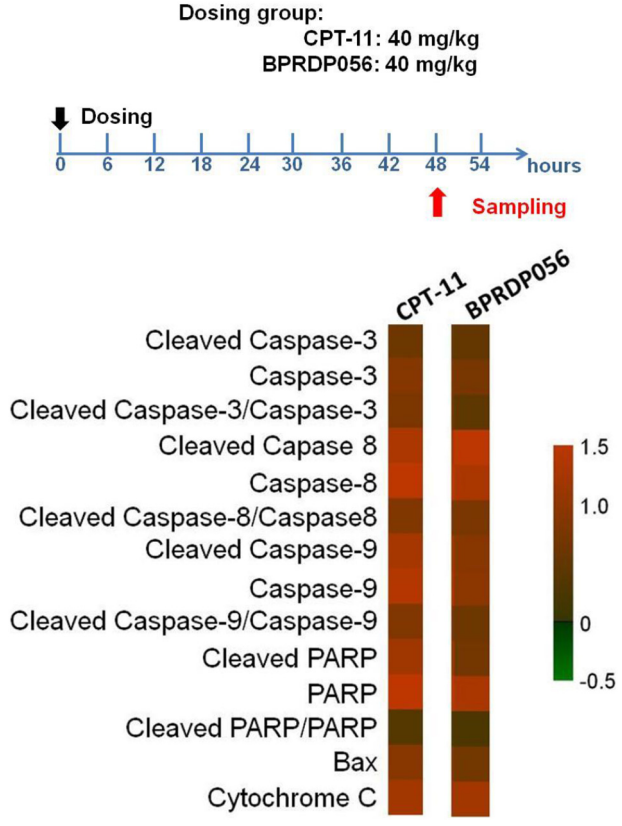

Fig. 5. Expression levels of the proteins related to cell death in BPRDP056-treated pancreatic MIA PaCa-2 tumors analyzed by micro-Western array. The heat map chart shows protein abundance in the tumors harvested at 48 h after the compound administration from the nude mice treated with BPRDP056 (40 mg/kg) and CPT-11 (40 mg/kg), which were normalized against the β-actin expression level and expressed in ratios to that of vehicle control. Red and green indicate increase and decrease, respectively, in the expression levels of proteins compared to that of vehicle control.

when formed a complex with PS on cancer cells and tumor vessel endothelium [23,24]. The combinations of pemetrexed, carboplatin, or docetaxel with bavituximab in clinical trials, however, have behaved similarly to pemetrexed/carboplatin/docetaxel alone [25–27]. To select patients stratified with the serum levels of β2GP1, a glycoprotein required for bavituximab targeting of PS, and thus to identify a subset of patients likely to benefit from the treatments of bavituximab has been suggested for its future clinical study design. Recently, a PS-targeting protein-drug conjugate (PDC) designed by fusing PS-binding synaptotagmin 1 (Syt1) C2A domains to a fusion of human IgG1-derived Fc fragments that are conjugated with 4 toxic monomethyl auristatin E (MMAE) molecules to the hinge cysteines of the Fc fusion [28]. The cytotoxic MMAE agent on the PDC is efficiently delivered and exhibits potent antitumor activities against xenograft tumors in mice [28]. Therefore, PS is a promising biomolecule for tumor site-specific targeting therapy to which SMDC may provide another strategy for PS targeting cancer therapy.

BPRDP056 is the first PS-targeting SMDC here reported with optimal drug-like properties and a broad spectrum of anticancer activities. BPRDP056 consists of three parts; Zn-DPA served as an anchoring group to target PS, payload topoisomerase I inhibitor SN38 active against tumor growth and the non-active spacer-bridging moiety between Zn-DPA and SN38. Zn-DPA coordination complexes are well known for their potent association with PS [11]. Our previous PS-association studies with DPA had shown that the linker and payload drug modifications on the Zn-DPA structure did not alter its PS binding ability *in vitro* [29]. The present study results indicate that the PS-specific targeting structure of BPRDP056 is essential for its anticancer activities in animals. As a PS-targeting into the tumor site, BPRDP056 achieved greater antitumor efficacies compared to CPT-11 in inhibiting the growth of xenograft human tumors of colorectal, pancreatic and breast cancer cells in mice. BPRDP060 comprised of the same PS-targeting Zn-DPA and linker moieties of BPRDP056 without the active SN38 payload and does not exhibit antitumor activities. Furthermore, the non-PS-targeting compound BPRDP067 conjugated with SN38 payload is the chemical structure analog of BPRDP056 and still lacks of any *in vivo* activity against tumor growth in nude mice. Therefore, both the tumor-targeting Zn-DPA and active SN38 payload in BPRDP056 are essential for its *in vivo* anticancer activities.

To achieve the combinatorial synergism between the PS-targeting approach and the payload releasing linker design the conjugate shall maintain stable as possibly be in the systemic circulation. Therefore, *in vitro* plasma stability and thus *in vivo* circulation stability of the conjugate is one of the important pharmacokinetic parameters for the design of SMDCs. In the pharmacokinetic study in mice and rat, AUC for BPRDP056 showed a longer stability of the conjugate in circulation. In previous pharmacokinetic studies from literature and tumor-bearing mice PK study in the present study, the results showed that the plasma concentration of SN38 which is the major metabolite of CPT-11 gave a log-linear decrease [30]. CPT-11 has a large CL and theoretical V_{ss} of pharmacokinetic parameter *in vivo* [31,32]. A large V_{ss} may indicate rapid and extensive uptake into most tissues which may lead to an off-target toxicity for a cancer chemotherapeutics. However, the V_{ss} for BPRDP056 injection was small indicating that the concentration of BPRDP056 in plasma circulation was great. Moreover, the mean plasma AUC for SN38 after the administration of BPRDP056 was high. The present study was further to compared to previous study [21]. A compound 13 is another novel PS-targeting drug conjugate. However, the pharmacokinetics profiling of BPRDP056 was improved compared to compound 13. The pharmacokinetic parameter of CL and V_{ss} trended to decrease and AUC significantly increased compared to compound 13. In the present study, AUC ratio ($AUC_{SN38}/AUC_{BPRDP056}$) of BPRDP056 was over than 40 folds [21]. In conclusion, BPRDP056 could slow down the elimination of SN38 and thereby extend the systemic circulation of BPRDP056 and SN38 in the blood.

The antitumor efficacy spectrum of BPRDP056 is here demonstrated significant against human tumors of pancreas cancer, prostate cancer, colon cancer, liver cancer, breast cancer and glioblastoma. With the same level of doses given, BPRDP056 and CPT-11 exhibited potent tumor growth inhibition activities, in which the conjugate BPRDP056 has only loaded

18% of SN38, whereas CPT-11 consists of 58% of SN38, in terms of the molecular weight fraction of SN38 in BPRDP056 and CPT-11, respectively. Tumor shrinkage was observed in the BPRDP056 treated mice subcutaneously and orthotopically bearing tumors at a lower payload dose of SN38 and better antitumor growth activities with the same dosing schedule. BPRDP056 show activities significantly superior to that of paclitaxel, CPT-11, sorafenib and comparable to that of temozolomide on inhibiting the human tumor growths (Fig. 3). Our observations provide strong evidence that the tumor-targeting Zn-DPA and SN38 on BPRDP056 are both essential for antitumor activities and a low dose of cytotoxic SN38 payload delivered by BPRDP056 achieves improved and prolonged antitumor efficacies in animals. The anticancer activity spectrum of BPRDP056 is broad and most likely to cover the tumors in which the levels of the targeted PS are high in tumor microenvironments.

Apoptosis can be triggered by external receptor-dependent stimuli or internal mitochondria-mediated signaling [33,34]. In the extrinsic pathway, activated caspase-8 can directly cleave and activate caspase-3, thus promoting apoptosis [35,36]. On the other hand, the intrinsic apoptotic pathway is modulated by sensing different types of cell stress followed by activation of Bax/Bak signaling machineries at the mitochondrial outer membrane [37], resulting in increase of the membrane permeability and release of cytochrome C, which activates caspase-9 [38]. Caspase-9 then cleaves and activates caspase-3 and consequent PARP cleavage, thus triggering apoptotic cell death [38,39]. Both extrinsic and intrinsic pathways interface at the caspase-3 activation [40].

Through micro-Western analysis of pancreatic MIA PaCa-2 tumors, the expression level of several proteins involved in apoptosis signaling events were examined. The levels of the extrinsic or internal apoptotic factors, such as caspase-3, caspase-8, caspase-9, and PARP, cytochrome C and Bax were found to be significantly increased. Further, BPRDP056 exhibited apoptotic signal levels similar to CPT-11 in the tumors harvested from the treated mice. Since BPRDP056 appears to exert the same antitumor mechanism of action as the topoisomerase I inhibitor SN38, the active moiety of both BPRDP056 and CPT-11. Observation of apoptosis profile of BPRDP056 has been verified on a prototype compound for proof of the concept [21]. Briefly, BPRDP056 delivered and concentrated SN38 could more efficiently trigger apoptotic cascade *in situ*, leading to sites specific higher exposure of PS from the inner membrane of cancer cells and tumor vessel endothelium in tumor microenvironment and subsequent facilitated recruitment more BPRDP056 from circulation through the Zn-DPA and PS association and resulted in antitumor efficacy. Since BPRDP056 showed a longer stability of the conjugate in circulation, BPRDP056 could slow down the elimination of SN38 and thereby extend the topoisomerase I inhibitor effect of SN38. In addition, the amount of SN38 in BPRDP056 was relatively lower than CPT-11 did at the same dosage administered. Furthermore, a previous study reported that antibodies targeting PS and blocking PS-mediated immunosuppression may be a novel approach to enhance immune responses against cancer [41]. Whether BPRDP056 has the ability to enhance the immune responses *via* binding to PS and thus against cancerous diseases remains to be investigated.

In conclusion, BPRDP056 is an entirely new innovative and first-in-class anti-cancer SMDC in biomolecule-targeted drug conjugate field. Instead of barriers and challenges associated with ADC development, BPRDP056 offers a good example of tumor site-selective delivery of a drug payload. BPRDP056 brings a good systemic stability in circulation and a slow clearance mechanism *in vivo* to shrink tumors at significantly reduced dosages of drug payload. The PS-specific targeted delivery system of BPRDP056 will be expected to cover the whole spectrum of tumor types with extracellular PS enriched in the tumor microenvironments. In this study, BPRDP056 has shown good potentials as a development drug candidate that provides therapeutic advantages over the current standard-of-care drugs.

CRediT authorship contribution statement

Yun-Yu Chen: Methodology, Investigation, Visualization, Validation, Chen-Fu Lo: Investigation, Validation, Tai-Yu Chiu: Visualization, Methodology, Validation, Software Writing-original draft preparation, Chia-Yu Hsu: Formal analysis, Methodology, Visualization, Software Writing-original draft preparation, Teng-Kuang Yeh: Methodology, Formal analysis, Resources, Writing-reviewing and editing, Ching-Ping Chen: Investigation, Chen-Lung Huang: Investigation, Chung-Yu Huang: Investigation, Min-Hsien Wang: Investigation, Yu-Chen Huang: Investigation, Hsuan-Hui Ho: Visualization, Yu-Sheng Chao: Conceptualization, Funding acquisition, Supervision, Joe C. Shih: Funding acquisition, Supervision, Lun K. Tsou: Methodology, Investigation, Project administration, Supervision, and Chiung-Tong Chen: Conceptualization, Resources, Data curation, Writing-reviewing and editing, Project administration, Funding acquisition, Supervision.

Declaration of competing interest

The authors declare the following financial interests/personal relationships which may be considered as potential competing interests: A patent (international application number: PCT/US2015/031386) has been filed in relation to this work. The authors, Y.S.C., L.K.T., and C.T.C, are also co-inventors in the patent. The authors declare no additional competing financial interests.

Acknowledgements

This work was supported by the grants from the National Health Research Institutes, the Ministry of Economic Affairs of Taiwan (MOEA 101-EC-17-A-22-1099, 102-EC-17-A-22-1099, 103-EC-17-A-22-1099, 104-EC-17-A-22-1099), and the Ministry of Health and Welfare of Taiwan (MOHW BP-101-PP, BP-102-PP, BP-103-PP, BP-104-PP).

References

[1] R.L. Siegel, K.D. Miller, A. Jemal, Cancer statistics, 2017, CA Cancer J. Clin. 67 (2017) 7–30.
[2] R.V. Chari, M.L. Miller, W.C. Widdison, Antibody-drug conjugates: an emerging concept in cancer therapy, Angew. Chem. Int. Ed. Engl. 53 (2014) 3796–3827.
[3] R.S. Zolot, S. Basu, R.P. Million, Antibody-drug conjugates, Nat. Rev. Drug Discov. 12 (2013) 259–260.
[4] G.D. Lewis Phillips, G. Li, D.L. Dugger, L.M. Crocker, K.L. Parsons, E. Mai, W.A. Blattler, J.M. Lambert, R.V. Chari, R.J. Lutz, W.L. Wong, F.S. Jacobson, H. Koeppen, R.H. Schwall, S.R. Kenkare-Mitra, S.D. Spencer, M.X. Sliwkowski, Targeting HER2-positive breast cancer with trastuzumab-DM1, an antibody-cytotoxic drug conjugate, Cancer Res. 68 (2008) 9280–9290.
[5] G. Casi, D. Neri, Antibody-drug conjugates and small molecule-drug conjugates: opportunities and challenges for the development of selective anticancer cytotoxic agents, J. Med. Chem. 58 (2015) 8751–8761.
[6] P. Polakis, Antibody drug conjugates for cancer therapy, Pharmacol. Rev. 68 (2016) 3–19.
[7] J.D. Bargh, A. Isidro-Llobet, J.S. Parker, D.R. Spring, Cleavable linkers in antibody-drug conjugates, Chem. Soc. Rev. 48 (2019) 4361–4374.
[8] N. Krall, J. Scheuermann, D. Neri, Small targeted cytotoxics: current state and promises from DNA-encoded chemical libraries, Angew. Chem. Int. Ed. Engl. 52 (2013) 1384–1402.
[9] A. Kumar, T. Mastren, B. Wang, J.T. Hsieh, G. Hao, X. Sun, Design of a small-molecule drug conjugate for prostate cancer targeted theranostics, Bioconjug. Chem. 27 (2016) 1681–1689.
[10] M. Srinivasarao, C.V. Galliford, P.S. Low, Principles in the design of ligand-targeted cancer therapeutics and imaging agents, Nat. Rev. Drug Discov. 14 (2015) 203–219.
[11] B.A. Smith, B.D. Smith, Biomarkers and molecular probes for cell death imaging and targeted therapeutics, Bioconjug. Chem. 23 (2012) 1989–2006.
[12] B.A. Smith, S. Xiao, W. Wolter, J. Wheeler, M.A. Suckow, B.D. Smith, In vivo targeting of cell death using a synthetic fluorescent molecular probe, Apoptosis 16 (2011) 722–731.
[13] R.G. Hanshaw, B.D. Smith, New reagents for phosphatidylserine recognition and detection of apoptosis, Bioorg. Med. Chem. 13 (2005) 5035–5042.
[14] D.R. Rice, K.J. Clear, B.D. Smith, Imaging and therapeutic applications of zinc(II)-dipicolylamine molecular probes for anionic biomembranes, Chem. Commun. (Camb.) 52 (2016) 8787–8801.
[15] A.V. Koulov, K.A. Stucker, C. Lakshmi, J.P. Robinson, B.D. Smith, Detection of apoptotic cells using a synthetic fluorescent sensor for membrane surfaces that contain phosphatidylserine, Cell Death Differ. 10 (2003) 1357–1359.
[16] B.A. Smith, W.J. Akers, W.M. Leevy, A.J. Lampkins, S. Xiao, W. Wolter, M.A. Suckow, S. Achilefu, B.D. Smith, Optical imaging of mammary and prostate tumors in living animals using a synthetic near infrared zinc(II)-dipicolylamine probe for anionic cell surfaces, J. Am. Chem. Soc. 132 (2010) 67–69.

[17] M. Aoki, A. Odani, K. Ogawa, Development of radiolabeled bis(zinc(II)-dipicolylamine) complexes for cell death imaging, Ann. Nucl. Med. 33 (2019) 317–325.

[18] Y. Kawato, M. Aonuma, Y. Hirota, H. Kuga, K. Sato, Intracellular roles of SN-38, a metabolite of the camptothecin derivative CPT-11, in the antitumor effect of CPT-11, Cancer Res. 51 (1991) 4187–4191.

[19] N.J. Chiang, T.Y. Chao, R.K. Hsieh, C.H. Wang, Y.W. Wang, C.G. Yeh, L.T. Chen, A phase I dose-escalation study of PEP02 (irinotecan liposome injection) in combination with 5-fluorouracil and leucovorin in advanced solid tumors, BMC Cancer 16 (2016) 907.

[20] C.S. Tsai, J.W. Park, L.T. Chen, Nanovector-based therapies in advanced pancreatic cancer, J. Gastrointest. Oncol. 2 (2011) 185–194.

[21] Y.W. Liu, Y.Y. Chen, C.Y. Hsu, T.Y. Chiu, K.L. Liu, C.F. Lo, M.Y. Fang, Y.C. Huang, T.K. Yeh, K.Y. Pak, B.D. Gray, T.A. Hsu, K.H. Huang, C. Shih, K.S. Shia, C.T. Chen, L.K. Tsou, Linker optimization and therapeutic evaluation of phosphatidylserine-targeting zinc dipicolylamine-based drug conjugates, J. Med. Chem. 62 (2019) 6047–6062.

[22] B. Sharma, S.S. Kanwar, Phosphatidylserine: a cancer cell targeting biomarker, Semin. Cancer Biol. 52 (2018) 17–25.

[23] I. Stasi, F. Cappuzzo, Profile of bavituximab and its potential in the treatment of non-small-cell lung cancer, Lung Cancer (Auckl.) 5 (2014) 43–50.

[24] T.A. Luster, J. He, X. Huang, S.N. Maiti, A.J. Schroit, P.G. de Groot, P.E. Thorpe, Plasma protein beta-2-glycoprotein 1 mediates interaction between the anti-tumor monoclonal antibody 3G4 and anionic phospholipids on endothelial cells, J. Biol. Chem. 281 (2006) 29863–29871.

[25] D.E. Gerber, D.R. Spigel, D. Giorgadze, M. Shtivelband, O.V. Ponomarova, J.S. Shan, K.B. Menander, C.P. Belani, Docetaxel combined with bavituximab in previously treated, advanced nonsquamous non-small-cell lung cancer, Clin. Lung Cancer 17 (2016) 169–176.

[26] J.E. Grilley-Olson, J. Weiss, A. Ivanova, L.C. Villaruz, D.T. Moore, T.E. Stinchcombe, C. Lee, J.S. Shan, M.A. Socinski, Phase Ib study of bavituximab with carboplatin and pemetrexed in chemotherapy-naive advanced nonsquamous non-small-cell lung cancer, Clin. Lung Cancer 19 (2018) e481–e487.

[27] D.E. Gerber, L. Horn, M. Boyer, R. Sanborn, R. Natale, R. Palmero, P. Bidoli, I. Bondarenko, P. Germonpre, D. Ghizdavescu, A. Kotsakis, H. Lena, G. Losonczy, K. Park, W.C. Su, M. Tang, J. Lai, N.L. Kallinteris, J.S. Shan, M. Reck, D.R. Spigel, Randomized phase III study of docetaxel plus bavituximab in previously treated advanced non-squamous non-small-cell lung cancer, Ann. Oncol. 29 (2018) 1548–1553.

[28] R. Li, S. Chiguru, L. Li, D. Kim, R. Velmurugan, D. Kim, S.C. Devanaboyina, H. Tian, A. Schroit, R.P. Mason, R.J. Ober, E.S. Ward, Targeting phosphatidylserine with calcium-dependent protein-drug conjugates for the treatment of cancer, Mol. Cancer Ther. 17 (2018) 169–182.

[29] Y.W. Liu, K.S. Shia, C.H. Wu, K.L. Liu, Y.C. Yeh, C.F. Lo, C.T. Chen, Y.Y. Chen, T.K. Yeh, W.H. Chen, J.J. Jan, Y.C. Huang, C.L. Huang, M.Y. Fang, B.D. Gray, K.Y. Pak, T.A. Hsu, K.H. Huang, L.K. Tsou, Targeting tumor associated phosphatidylserine with new zinc dipicolylamine-based drug conjugates, Bioconjug. Chem. 28 (2017) 1878–1892.

[30] N. Kaneda, T. Yokokura, Nonlinear pharmacokinetics of CPT-11 in rats, Cancer Res. 50 (1990) 1721–1725.

[31] C. Wu, Y. Zhang, D. Yang, J. Zhang, J. Ma, D. Cheng, J. Chen, L. Deng, Novel SN38 derivative-based liposome as anticancer prodrug: an in vitro and in vivo study, Int. J. Nanomedicine 14 (2019) 75–85.

[32] N. Kaneda, H. Nagata, T. Furuta, T. Yokokura, Metabolism and pharmacokinetics of the camptothecin analogue CPT-11 in the mouse, Cancer Res. 50 (1990) 1715–1720.

[33] J.M. Adams, Ways of dying: multiple pathways to apoptosis, Genes Dev. 17 (2003) 2481–2495.

[34] G. Kroemer, L. Galluzzi, C. Brenner, Mitochondrial membrane permeabilization in cell death, Physiol. Rev. 87 (2007) 99–163.

[35] A. Strasser, L. O'Connor, V.M. Dixit, Apoptosis signaling, Annu. Rev. Biochem. 69 (2000) 217–245.

[36] A. Ashkenazi, Targeting death and decoy receptors of the tumour-necrosis factor superfamily, Nat. Rev. Cancer 2 (2002) 420–430.

[37] M.C. Wei, W.X. Zong, E.H. Cheng, T. Lindsten, V. Panoutsakopoulou, A.J. Ross, K.A. Roth, G.R. MacGregor, C.B. Thompson, S.J. Korsmeyer, Proapoptotic BAX and BAK: a requisite gateway to mitochondrial dysfunction and death, Science 292 (2001) 727–730.

[38] P. Li, D. Nijhawan, I. Budihardjo, S.M. Srinivasula, M. Ahmad, E.S. Alnemri, X. Wang, Cytochrome c and dATP-dependent formation of Apaf-1/caspase-9 complex initiates an apoptotic protease cascade, Cell 91 (1997) 479–489.

[39] A.H. Boulares, A.G. Yakovlev, V. Ivanova, B.A. Stoica, G. Wang, S. Iyer, M. Smulson, Role of poly(ADP-ribose) polymerase (PARP) cleavage in apoptosis. Caspase 3-resistant PARP mutant increases rates of apoptosis in transfected cells, J. Biol. Chem. 274 (1999) 22932–22940.

[40] V. Nikoletopoulou, M. Markaki, K. Palikaras, N. Tavernarakis, Crosstalk between apoptosis, necrosis and autophagy, Biochim. Biophys. Acta 1833 (2013) 3448–3459.

[41] O. Belzile, X. Huang, J. Gong, J. Carlson, A.J. Schroit, R.A. Brekken, B.D. Freimark, Antibody targeting of phosphatidylserine for the detection and immunotherapy of cancer, Immunotargets Ther. 7 (2018) 1–14.